CHAPTER 2 HIGHLY ANGULARLY STABLE DUAL-BANDSTOP FSS FOR BLOCKING SATELLITE DOWNLINK FREQUENCIES*

*Part of this work has been published as:

G. Venkatesh, M. Thottappan and S. P. Singh, "Highly Angularly Stable Dual-Band Stop FSS for Blocking Satellite Downlink Frequencies," in *IEEE Transactions on Electromagnetic Compatibility*, vol. 64, no. 6, pp. 2055-2059, Dec. 2022, doi: 10.1109/TEMC.2022.3200212

2.1. Introduction

In [64], a dual-band FSS is documented for shielding GSM signals. Meanwhile, [40] introduces the design of a dual-band quarter ring FSS tailored for Wi-Fi applications. Another noteworthy mention in [41] discusses an FSS-based band-stop filter effective in blocking WiMAX, WLAN, and X-band signals. Closely spaced frequency response dual-band filters, reported in [49], [66] and [50]. Literature reveals various proposals for dual-band stop FSSs aimed at blocking diverse microwave frequencies. This chapter introduces a novel approach by designing a dual band-stop FSS to block satellite downlink frequencies. Achieving higher angular stability, a simple straight-line structure is employed instead of more intricate designs. The proposed dual bandstop FSS filter aims to block satellite downlink frequencies in both C-band (3.7-4.2 GHz) and X-band (7.25-7.75 GHz).

A stable resonant frequency concerning the angle of incidence is achieved with small inter-element spacing, indicating higher periodicity (as mentioned in [1]). The angular stability of high periodic structures at larger angles of incidence relies on the unit-cell's structure.

For enhanced angular stability, a single-element unit-cell structure is favored over a dual-element structure (which yields two resonant frequencies). Mutual impedance between elements in the dual-element structure may hinder achieving higher angular stability. In [67], a dual-band FSS with concentric circular loops is presented, but its angular stability is limited. References [42], [43] and [92] document single-band structures with high angular stability. For dual-band angular stability, a convoluted structure is introduced in [93], and [94-96] explore the use of two-layered structures and vias, that increases the complexity of the structure. In this chapter, a simple straight line structure is proposed, aiming to provide a balance between simplicity and the desired angular stability.

The novelty of the structure lies in its design: a single pair of dipoles (horizontal and vertical) with two folded arms, designed to stop two frequency bands for both TE and TM polarizations. The structure provides good angular stability over a large range of incidence angles. The angular stability structures reported in [94], [95], and [96] are two-layer structures and/or use vias. The advantage of the proposed structure over these is its simplicity, which facilitates ease of fabrication and practical implementation.

To determine equivalent circuit parameters a new and distinct approach is adapted, enhancing the overall novelty and contribution of the research.

2.2. Proposed Structure

2.2.1. Unit-Cell Design

The inspiration for crafting the envisioned unit-cell stems from the widely recognized crossed dipole, particularly the crossed dipole with folded arms resembling a swastika shape. This configuration imparts a singular stopband resonance. The introduction of a second arm to the swastika-type structure has led to the current unit-cell design, capable of achieving dual stopband resonances. The proposed FSS unit cell contains both horizontal and vertical dipoles having two folded arms at their ends. The first arm is straight, while the second arm is extended into the interior of the unit cell as shown in Fig. 2.1. The substrate material used in the proposed structure is the commercially available FR-4 having a dielectric constant, ε_r of 4.4, the thickness of 1.6mm, and a loss tangent of 0.02. The resonant frequency of an FSS depends primarily on the dimensions of the individual elements. The basic type of elements resonate when the largest tip to tip electrical length is approximately equal to the half of the wavelength [1]. From this the initial dimensions of the structure are estimated. The unit cell of the proposed FSS bandstop filter is simulated by using 3D FEM-based Ansys HFSS. Using parametric analysis in HFSS the structure

parameters are optimized. The optimized dimensions of the proposed structure for obtaining the desired response are given in Table 2.1.

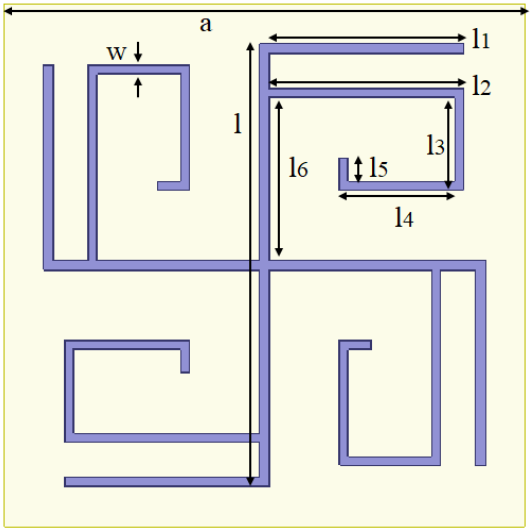

(a)

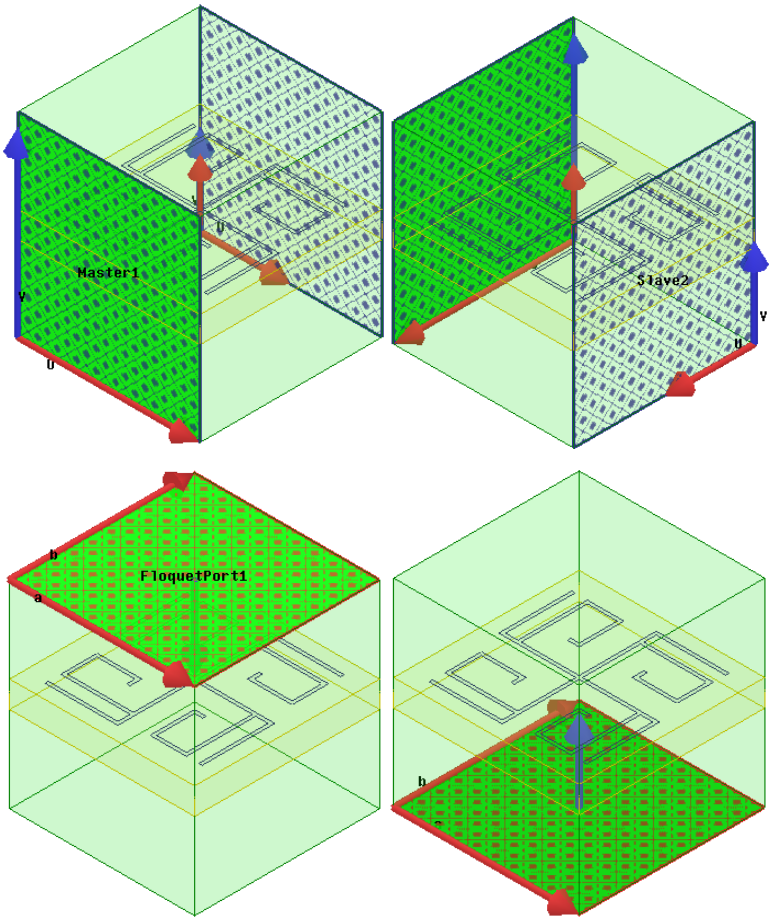

(b)

Fig. 2.1. (a) Unit cell geometry of the proposed FSS bandstop filter, (b) Simulation setup.

Table 2.1. Geometrical Parameter values of the Proposed FSS Unit-Cell.

Parameter	Value (mm)	Parameter	Value (mm)
a	11.2	l_3	2
w	0.2	l_4	2.5
l	9.5	l_5	0.5
l_1	4.2	l_6	3.5
l_2	4.2		

2.2.2. Simulated Results

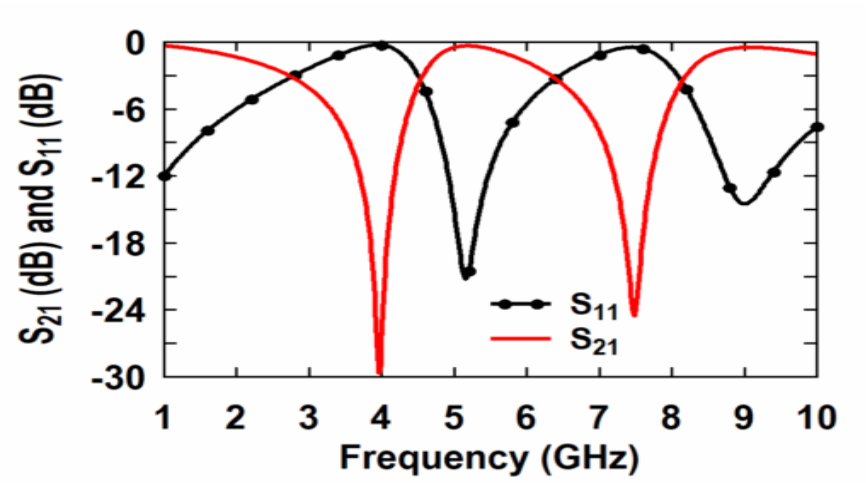

(a)

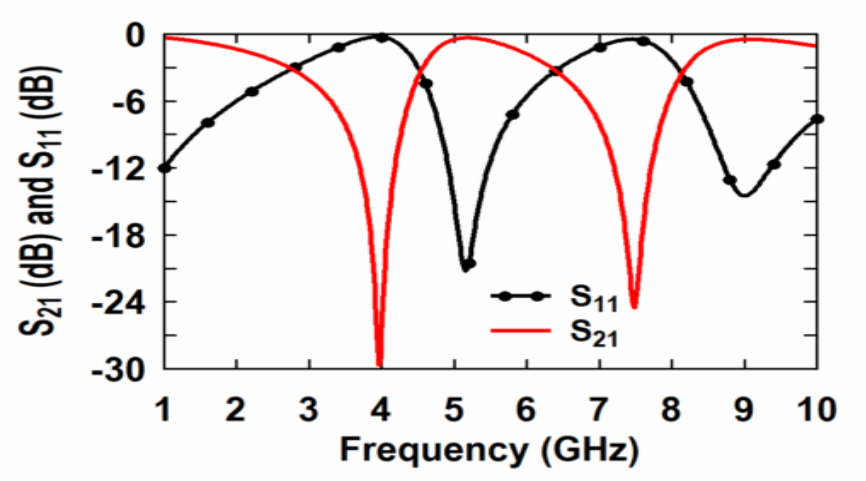

(b)

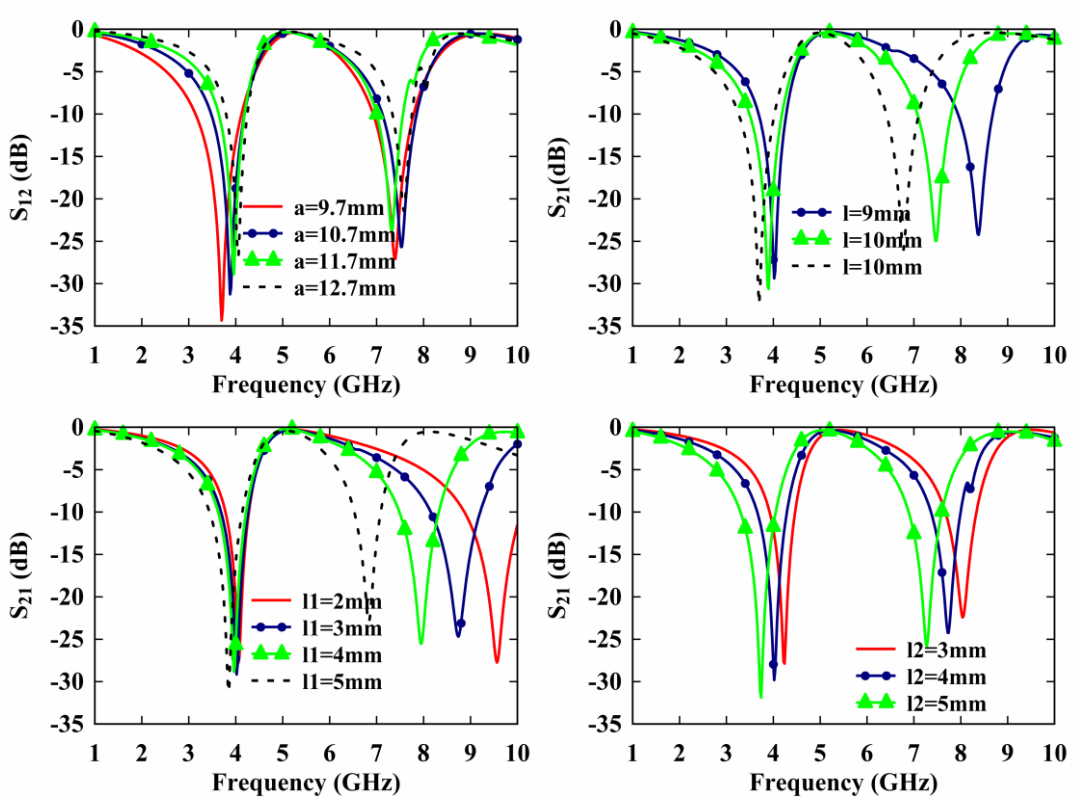

(c)

Fig. 2.2. Transmission coefficient- frequency characteristic of FSS filter at normal incidence for (a) TE polarization and (b) TM polarization. (c) Parametric analysis of the structure.

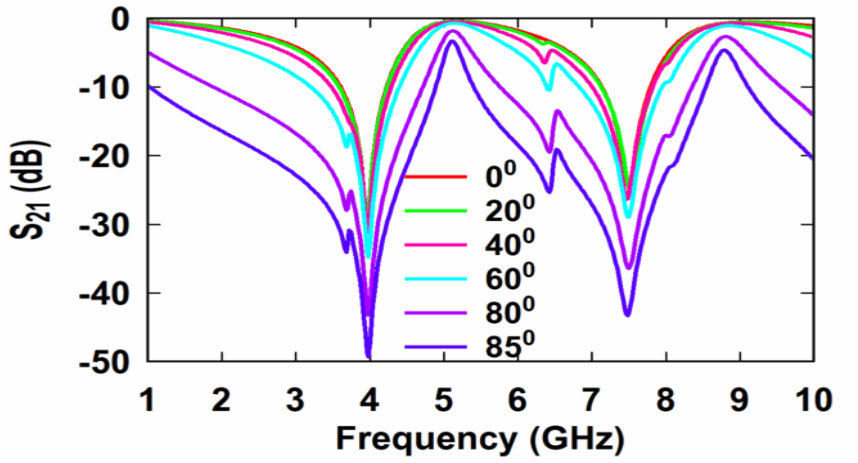

Fig. 2.3. Transmission-frequency characteristics of FSS filter at different angles of oblique incidence for TE polarization.

The simulation setup is given in Fig. 2.1 (b). The transmission coefficient (S_{21})-frequency characteristics of the structure at normal incidence for TE and TM polarizations are shown in Fig. 2.2. It can be seen that S_{21} values are below -10 dB for two satellite downlink frequency bands 3.7-4.2 GHz and 7.25-7.75 GHz for both TE and TM polarizations. The transmission coefficient (S_{21})-frequency characteristics of the structure for various incident angles are shown in Fig. 2.3 and Fig.2.4. The frequency response of the FSS filter is constant over a wide range of incident angles, i.e., up to 85^0 for both TE and TM polarizations. At higher oblique incident angles (such as 80^0 and 85^0) the bandwidth of the structure slightly varies but the structure gives stable resonant frequencies up to 85^0 of oblique incidence. Beyond 85°, the resonant frequency changes slightly for the reported structure, so the transmission characteristics are presented up to an 85° oblique incidence.

The resonant characteristics of the proposed structure can be understood through the induced surface current at two resonant frequencies of 3.96 and 7.5 GHz, as shown in Fig. 2.5. It is observed from Fig. 2.5 that the current flows in both horizontal and vertical dipoles at the resonant frequency of 3.96 GHz. In contrast, the current flows in the vertical dipole only at other resonant frequency of 7.5 GHz. Even though the proposed structure is designed for satellite downlink frequencies, by changing strip lengths and the distance between unit-cells the resonant frequencies and the bandwidth can be changed respectively (Fig.2.2 (c)). The proposed structure is single elemental unit-cell structure. For a single elemental structure instead of dual elemental structures (e.g., two circular loops or two square loops for two bands), achieving two specific resonant frequencies is more difficult because tuning one desired frequency by changing the structure's dimensions may lead to the detuning of the other desired frequency.

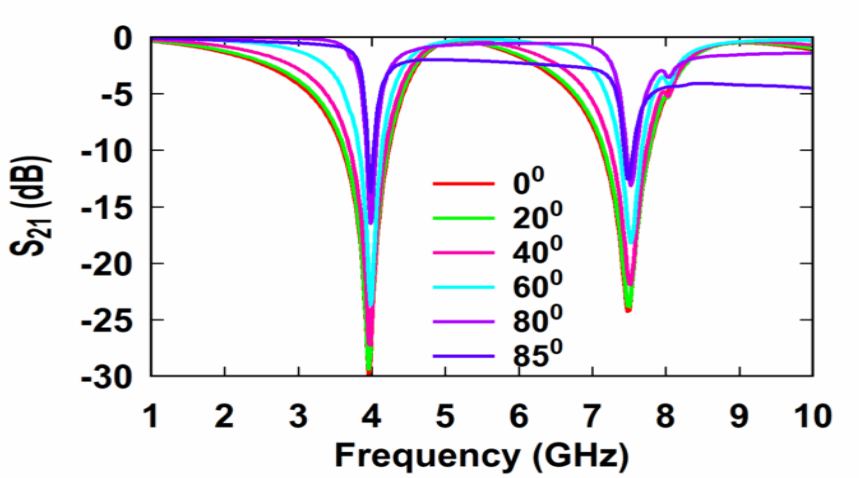

Fig. 2.4. Transmission-frequency characteristics of FSS filter at different angles of oblique incidence for TM polarization.

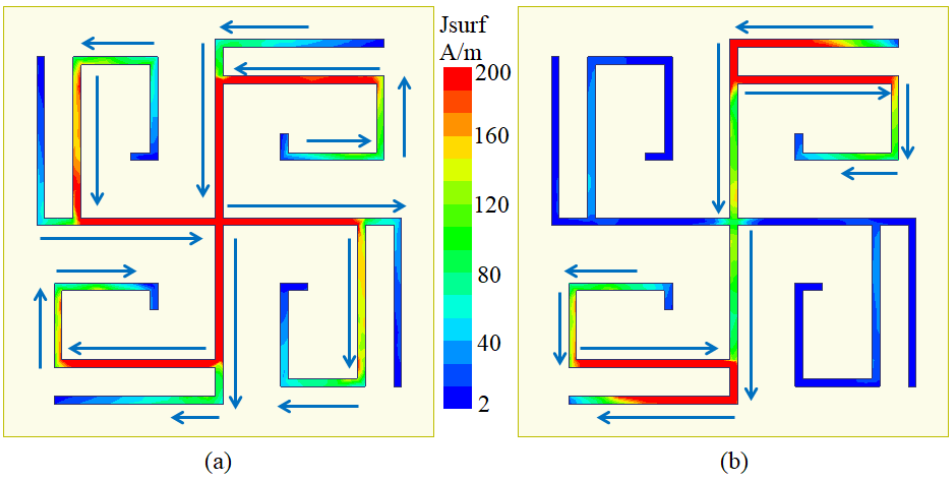

Fig. 2.5. Induced surface current of FSS at (a) 3.96GHz and (b) 7.5GHz.

2.3. Equivalent Circuit

The equivalent circuit of the unit cell can be drawn from the current and voltage distribution plots. The voltage distribution plot is given in Fig.2.6. The strip length and gap between the strips correspondence to inductance and capacitance are shown in Fig.2.7. The equivalent circuit of the unit cell of the proposed FSS at two resonant frequencies i.e. f_1 (=3.96 GHz) and f_2 (=7.5 GHz) are given in Fig.2.8 (a) and Fig. 2.8 (b) respectively. The simplified equivalent circuit of the structure is given in Fig. 2.8 (c).

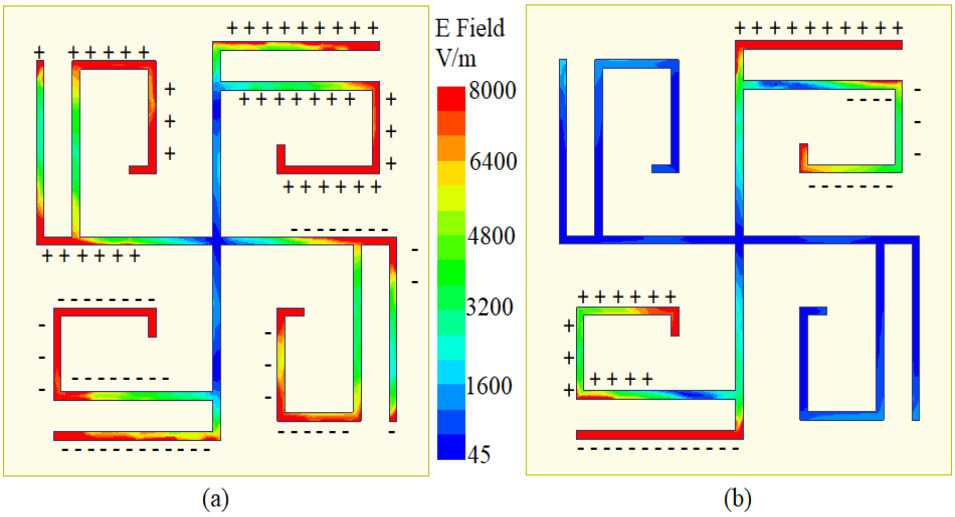

Fig. 2.6. Voltage distribution of FSS at (a) 3.96GHz and (b) 7.5GHz.

Equation (2.1) and (2.2) represents resonant frequency in terms of inductance and capacitance.

$$f_1 = \frac{1}{2\pi\sqrt{L_1 C_1}} \tag{2.1}$$

$$f_2 = \frac{1}{2\pi\sqrt{L_2 C_2}} \tag{2.2}$$

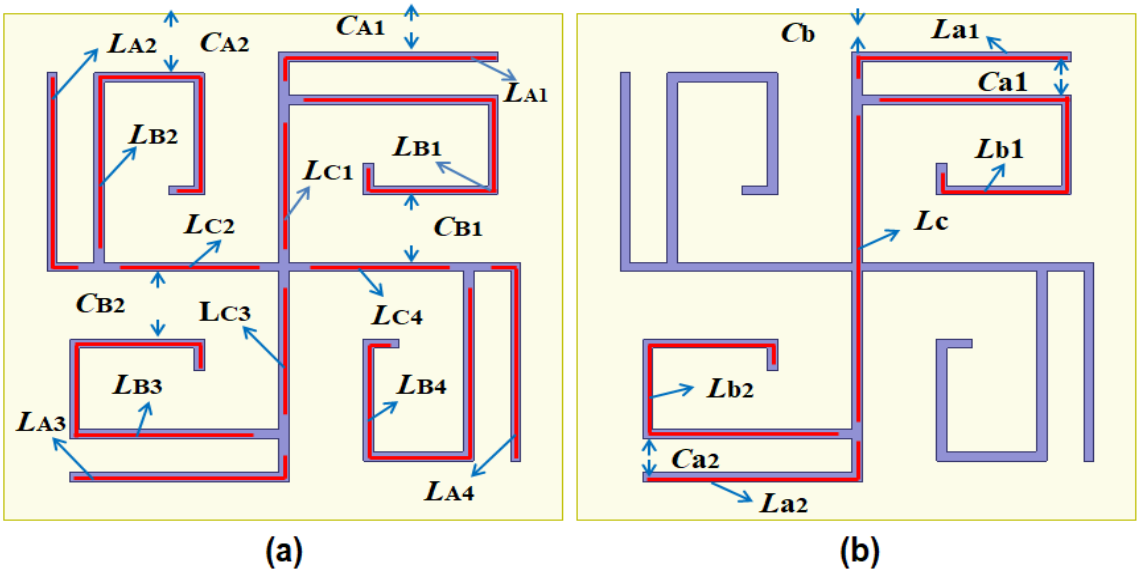

Fig. 2.7. Representation of equivalent circuit parameters of FSS at (a) 3.96GHz and (b) 7.5GHz.

Where, L_1, L_2, and C_1, C_2 are equivalent inductances and capacitances of the simplified equivalent circuit of the proposed FSS unit cell. Using equations (2.1) and (2.2), the inductances L_1 and L_2 can be written in terms of the capacitances C_1 and C_2. The capacitances C_1 and C_2 are calculated from the simulated transmission coefficient values at four different frequencies (3.7, 4.2, 7.2, and 7.8 GHz) by using a well-known transmission line relation, which is expressed in terms of ABCD parameters and Z_0 intrinsic impedance of free space [97]

$$\left.\begin{aligned} T(S_{21}) &= \frac{2Z_0}{AZ_0 + B + CZ_0^2 + DZ_0} \\ \begin{pmatrix} A & B \\ C & D \end{pmatrix} &= \begin{pmatrix} 1 & 0 \\ \dfrac{1}{Z_{FSS}} & 1 \end{pmatrix} \end{aligned}\right\} \tag{2.3}$$

Table 2.2. Final Parameter Values of FSS Structure

Parameter	Value (fF)	Parameter	Value (nH)
C_1	105	L_1	15.38
C_2	34	L_2	13.25

The calculated values of C_1 and C_2 are substituted in equation (2.3) to obtain the calculated frequency response (S21-frequency characteristic) of the structure in the frequency band 1-10 GHz. The calculated frequency response of the filter initially deviated from the simulated one. Therefore, the calculated values of C_1 and C_2 were changed to find the new calculated frequency response of the filter. This new calculated frequency response was compared with the simulated one again. This process was repeated till the calculated frequency response of the structure is nearly in agreement with the simulated one. Those calculated values of C_1 and C_2 were selected for which

the calculated frequency response nearly matched the simulated one in the frequency band of interest (Fig. 2.9). Once calculated values of C_1 and C_2 are known, the values of L_1 and L_2 can be easily determined using equations (2.1) and (2.2). The optimized values of each element in the equivalent circuit of the proposed FSS unit cell are given in Table 2.2.

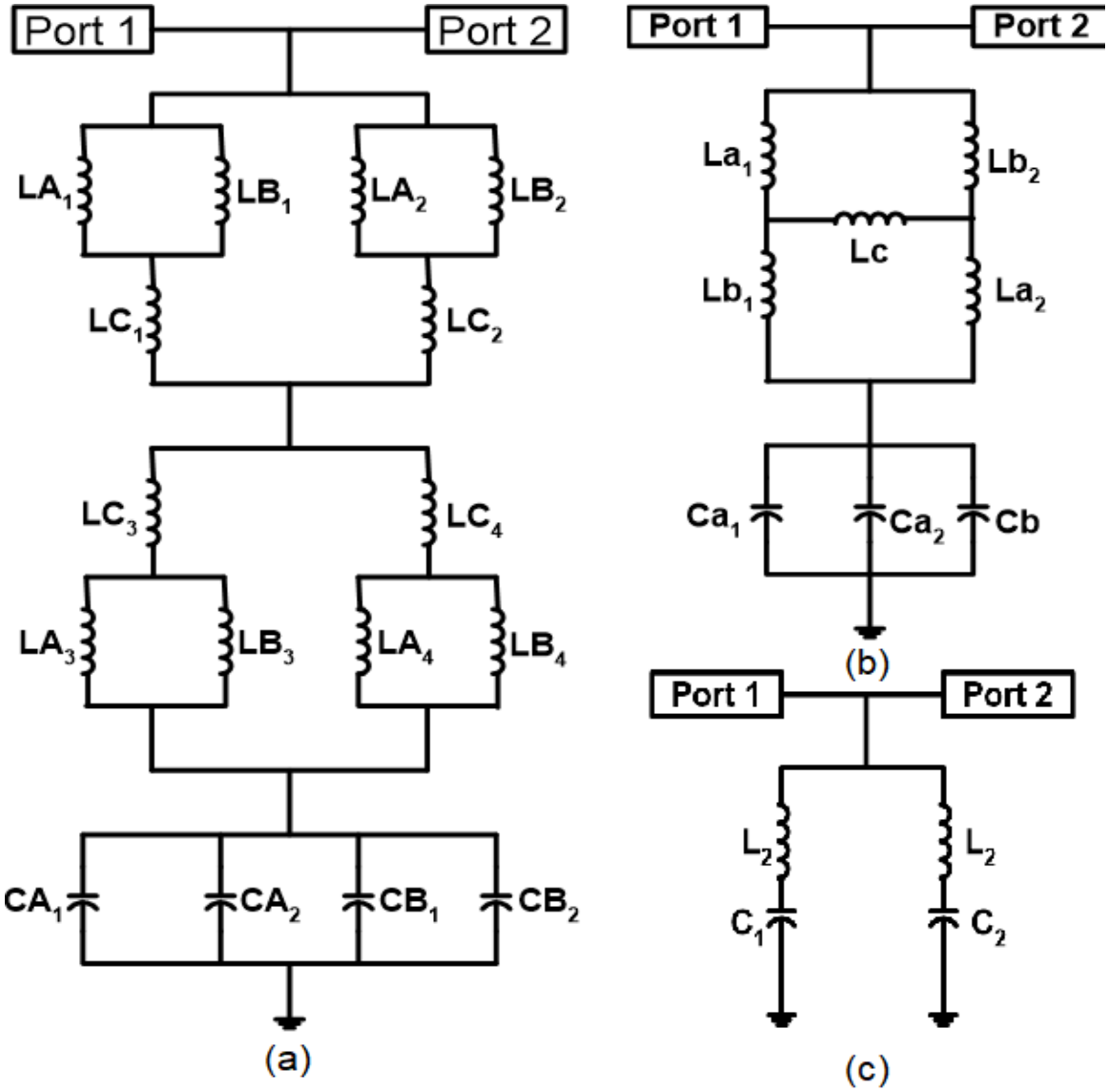

Fig. 2.8. Equivalent circuit of the proposed FSS unit cell (a) at 3.96 GHz. (b) at 7.5 GHz (c) simplified circuit.

Table 2.3. Comparison with the existing Simulated FSS structures

Ref.	FSS Structure	Application	Reported maximum angle of incidence
[64]	Modified double square loop elements	GSM Shielding	60^0
[40]	Circular loop with inner circular arcs	To stop Wi-Fi Signals	60^0
[41]	Window type lines enclosed by a square loop	WiMAX, WLAN, and X-Band filtering	50^0
[49]	Meander type lines	Dual stop-band at 2.54 GHz and 3.54 GHz	60^0
[66]	Square patch with strip lines at edges	Dual-frequency applications at X-band	60^0
[50]	Convoluted meandered pattern	Dual stop-band at 2.35 GHz, 3.05GHz	75^0
[67]	Circular loop with an inner split circular loop	To stop ISM signals	60^0
[42]	Rotated cross dipole	Single X- band	60^0
[43]	Combined two modified cross loops	Single stop-band at 8.7 GHz	85^0
[92]	Strong coupled FSS	Single stop-band at 2 GHz	84^0
[93]	Convoluted structure	Dual stop-band at 2.66 GHz and 5 GHz	60^0
[94]	Two layered Jerusalem Cross with meandering lines connected with vias	Dual sop-band at 2.4 GHz and 5GHz	85^0
[95]	Two layered meandered line structures connected with vias	Dual stop-band at 0.75 GHz and 1.8 GHz	85^0
[96]	Single layered cross dipole, meandering end loading dipole and vias	WLAN	85^0
present work	Single layered Dipoles with folded arms	To stop satellite downlink frequencies	85^0

2.4. Experimental Results

To verify the simulated results, a prototype of the proposed structure of 280 x 180 mm^2 with 25 x 16 elements is fabricated by CVD and etching process, as shown in Fig. 2.10. The fabricated structure is experimentally tested in a microwave anechoic chamber with two horn antennas and a VNA setup, as shown in Fig. 2.11. The structure is placed in the far-field region from the transmitting antenna and just in front of the receiving antenna to cover the entire aperture of the receiving antenna to measure better transmission characteristics of the structure. Fig. 2.9 shows that both simulated and measured frequency responses at normal incidence are found to be closely matching. Oblique incidence response of the proposed structure also has been measured and shown in Fig. 2.12 and Fig. 2.13, which shows the good angular stability of the proposed structure. Due to the fabrication tolerances (FSS array consist large number of elements, each element should be fabricated with exact same dimensions) and measurement limitations (structure surroundings are not covered by absorbing material) a small deviation has been observed.

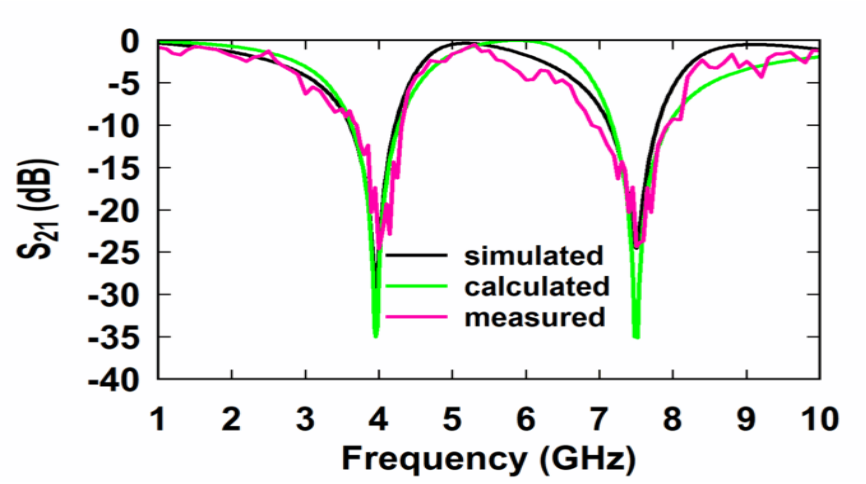

Fig.2.9. Simulated, calculated, and measured frequency response.

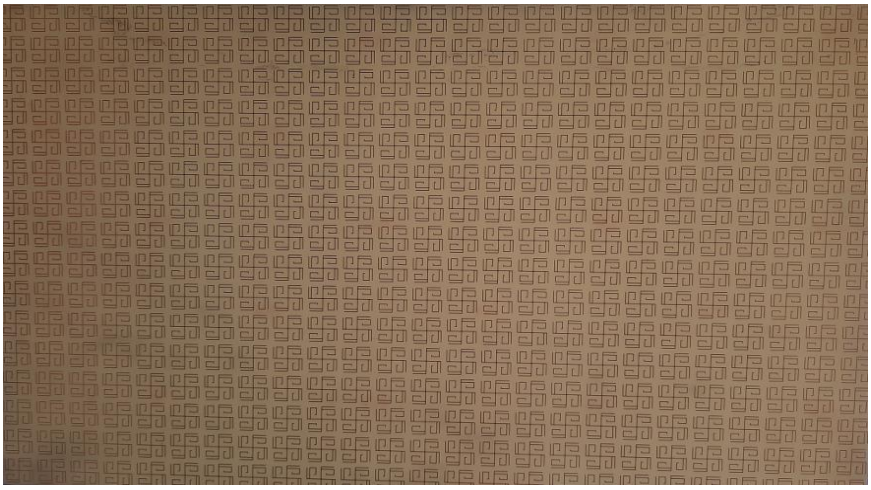

Fig. 2.10. Photograph of the fabricated structure.

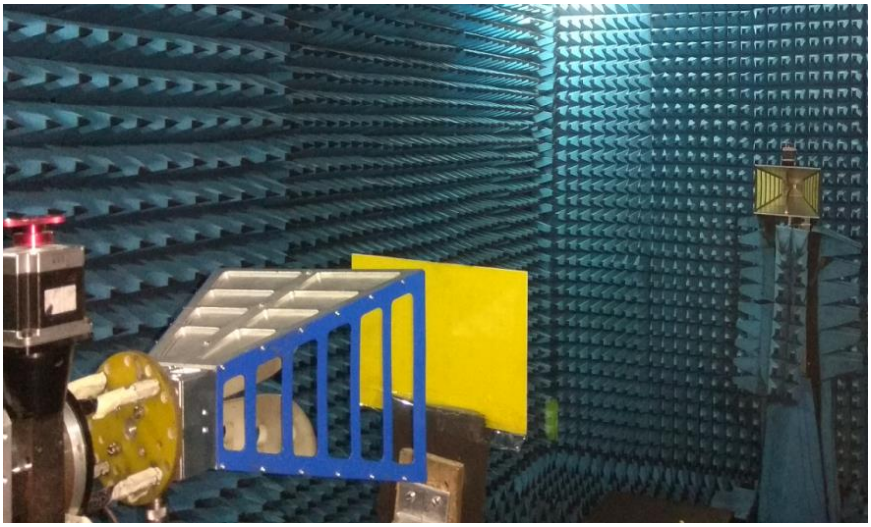

Fig. 2.11. Photograph of the measurement setup.

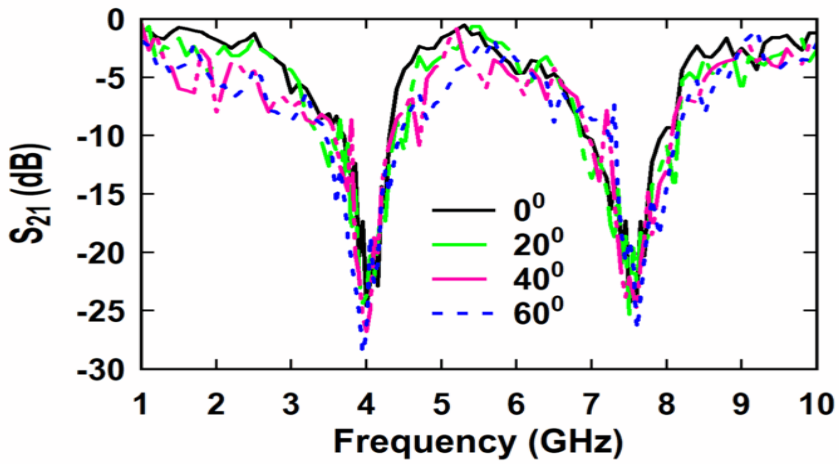

Fig. 2.12. Measured frequency response of the structure for TE polarization.

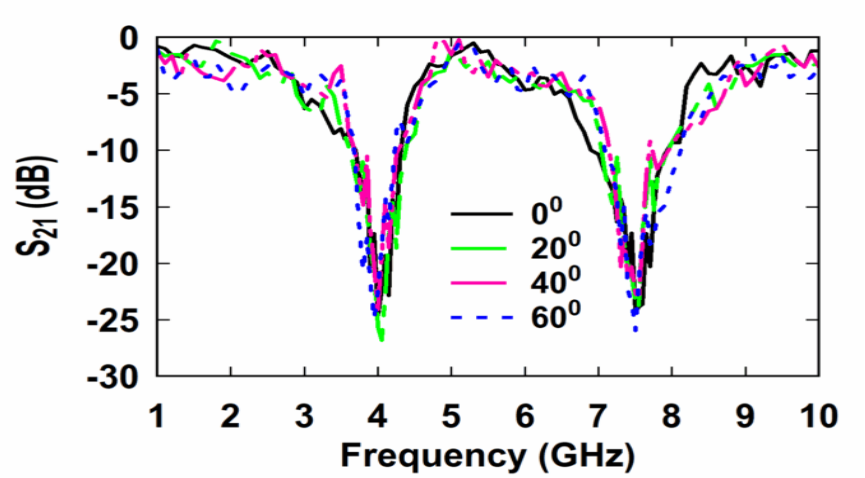

Fig.2. 13. Measured frequency response of the structure for TM polarization.

2.5. Conclusion

In this chapter, an FSS based dual-band stop filter for blocking the satellite downlink frequency bands has been reported. The proposed filter has been designed, simulated, fabricated, and experimentally verified. The proposed structure was studied and observed that it gives a stable frequency response for a large variation of incident angles for both TE and TM polarizations. The proposed dual-band was also observed that it has higher angular stability up to 85^0. Comparison of present work with previously reported structures is given in Table 2.3. The proposed FSS filter may very useful in potential applications like wireless communication and radar systems to improve their performances.